Editors' Suggestion

Emulating Quantum Teleportation of a Majorana Zero Mode Qubit

He-Liang Huang,[1,2,3,4,*] Marek Narożniak,[5,6,*] Futian Liang,[1,2,3,*] Youwei Zhao,[1,2,3] Anthony D. Castellano,[1,2,3] Ming Gong,[1,2,3] Yulin Wu,[1,2,3] Shiyu Wang,[1,2,3] Jin Lin,[1,2,3] Yu Xu,[1,2,3] Hui Deng,[1,2,3] Hao Rong,[1,2,3] Jonathan P. Dowling,[7,8,9] Cheng-Zhi Peng,[1,2,3] Tim Byrnes,[5,9,10,6] Xiaobo Zhu,[1,2,3,†] and Jian-Wei Pan[1,2,3]

[1]*Hefei National Laboratory for Physical Sciences at the Microscale and Department of Modern Physics, University of Science and Technology of China, Hefei 230026, China*

[2]*Shanghai Branch, CAS Center for Excellence in Quantum Information and Quantum Physics, University of Science and Technology of China, Shanghai 201315, China*

[3]*Shanghai Research Center for Quantum Sciences, Shanghai 201315, China*

[4]*Henan Key Laboratory of Quantum Information and Cryptography, Zhengzhou, Henan 450000, China*

[5]*New York University Shanghai, 1555 Century Ave, Pudong, Shanghai 200122, China*

[6]*Department of Physics, New York University, New York, New York 10003, USA*

[7]*Hearne Institute for Theoretical Physics, Department of Physics and Astronomy, Louisiana State University, Baton Rouge, Louisiana 70803, USA*

[8]*Hefei National Laboratory for Physical Sciences at Microscale and Department of Modern Physics, University of Science and Technology of China, Hefei, Anhui 230026, China*

[9]*NYU-ECNU Institute of Physics at NYU Shanghai, 3663 Zhongshan Road North, Shanghai 200062, China*

[10]*State Key Laboratory of Precision Spectroscopy, School of Physical and Material Sciences, East China Normal University, Shanghai 200062, China*

(Received 18 September 2020; revised 30 November 2020; accepted 14 January 2021; published 3 March 2021)

Topological quantum computation based on anyons is a promising approach to achieve fault-tolerant quantum computing. The Majorana zero modes in the Kitaev chain are an example of non-Abelian anyons where braiding operations can be used to perform quantum gates. Here we perform a quantum simulation of topological quantum computing, by teleporting a qubit encoded in the Majorana zero modes of a Kitaev chain. The quantum simulation is performed by mapping the Kitaev chain to its equivalent spin version and realizing the ground states in a superconducting quantum processor. The teleportation transfers the quantum state encoded in the spin-mapped version of the Majorana zero mode states between two Kitaev chains. The teleportation circuit is realized using only braiding operations and can be achieved despite being restricted to Clifford gates for the Ising anyons. The Majorana encoding is a quantum error detecting code for phase-flip errors, which is used to improve the average fidelity of the teleportation for six distinct states from $70.76 \pm 0.35\%$ to $84.60 \pm 0.11\%$, well beyond the classical bound in either case.

DOI: 10.1103/PhysRevLett.126.090502

One of the most attractive ways of performing fault-tolerant quantum computing [1–8] is topological quantum computing [9–15]. In topological quantum computing, the quantum information is stored in the states of anyons, which have a nontrivial effect on the total state when they are interchanged. The logical states of the anyons form a subspace distinguishing the error-free space to those with errors, and errors are suppressed via the topological gap. For non-Abelian anyons, their braiding can be used to construct elementary quantum gates for quantum computing. The resulting quantum gate is only dependent upon the topology of the braiding path; thus, small imperfections in the braiding can be tolerated as long as the operation is topologically equivalent.

One example of a non-Abelian anyon is the Majorana zero mode (MZM) [14,16–20]. MZMs are zero energy excitations that occur typically in low-dimensional topological superconductors. Two physical systems where MZMs have been intensely investigated are fractional quantum Hall systems [21–24] and semiconductor nanowires [25–27]. To date, many experiments have been conducted to find the evidence for the existence of Majorana fermions; however, the key feature of topological protection has not yet been demonstrated [28]. An elementary model that possesses MZMs is the Kitaev chain consisting of N fermions with Hamiltonian [16],

$$H = \sum_{n=1}^{N-1} \Delta(c_n c_{n+1} + c_{n+1}^{\dagger} c_n^{\dagger}) - t(c_{n+1}^{\dagger} c_n + c_n^{\dagger} c_{n+1}) - \mu c_n^{\dagger} c_n, \quad (1)$$

where c_n is a fermionic annihilation operator on site n, and t is the hopping energy, Δ is the superconducting gap, and μ is a chemical potential. For finite N and working in the limit $\Delta = t$ and $\mu = 0$, the model has a degenerate ground state, corresponding to the presence or absence of a pair of MZMs,

and can be used to encode the state of a qubit. By braiding one of the MZMs with another, quantum gates on the encoded quantum information may be performed, thereby forming the basis for topological quantum computing.

While the direct realization of topological quantum computing based on MZMs is still out of reach of present day technology, the study of the Majorana physics is now possible by way of quantum simulation in other controllable systems such as superconducting and ion-trap systems [29]. Mapping the Kitaev chain to a spin model via the Jordan-Wigner transformation, the Hamiltonian (1) takes the form of a one-dimensional transverse field Ising model, which has made it attractive to numerous proposals for simulating its equivalent dynamics. Xu, Pachos, and Guo implemented the spin version of MZMs states in a Kitaev chain, and braiding of the effective anyons was demonstrated to realize one qubit gates with imaginary time evolution [30,31]. Several works have also demonstrated the path-independent nature of braiding anyonic excitations in the toric code [32–37]. Simulating the physics of Majorana fermions by artificially constructed lattice models can provide additional insight into the nature of the quantum states, such as allowing one to tap into the existing pool of ideas on Majorana-based quantum computation [38,39]. To date, such studies have been restricted to examining the basic properties of anyons, and we are not aware of any quantum simulation of topological quantum computing involving more than one encoded qubit.

In this Letter, we investigate the feasibility of topological quantum computing by simulating the quantum teleportation [40] of a MZM state of the Kitaev chain on superconducting qubits. We realize four spin-mapped Kitaev chains using eight superconducting qubits (see Fig. 1). Each chain, consisting of two physical qubits, encodes a single logical qubit, corresponding to the spin-mapped MZM states. In the teleportation, Alice is in possession of two of the Kitaev chains, and Bob holds the two other chains. The teleportation then transfers a single logical qubit, encoded as the spin-mapped MZM states, from Alice to Bob. One of the well-known issues of quantum computing based on MZMs is that braiding operations only allow for a discrete number of Clifford gates, which is insufficient for universal quantum computation [11,41,42]. Fortunately, in the teleportation protocol, only Clifford gates are required, such that it can be completed entirely with braiding operations. In addition to demonstrating the feasibility of anyonic quantum computing, we also show the error protection capabilities of MZMs. The protection of quantum information via error correcting codes has been demonstrated in many past works [43–52], including those based on topological states [44,52]. We show that the spin-mapped MZM states are capable of detecting phase errors, allowing us to improve the teleportation fidelity significantly.

We first give a brief review of anyonic quantum computing with MZMs. Each fermion is written in terms of two Majoranas according to the definition

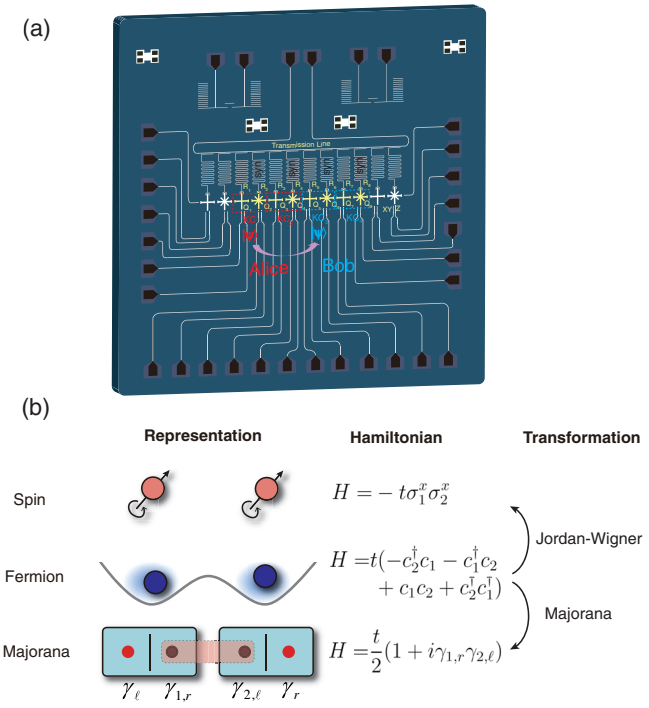

FIG. 1. Experimental configuration and the mapping of Kitaev chain to its spin and Majorana representations. (a) The superconducting quantum processor. We choose eight adjacent qubits labelled with Q_1 to Q_8 from the 12-qubit processor to perform the experiment. Qubits Q_1 to Q_4 and Q_5 to Q_8 are held by Alice and Bob, respectively. Pairs of qubits form a spin-mapped Kitaev chain (KC), each which encodes a single logical qubit. Each qubit couples to a resonator for state readout, marked by R_1 to R_8. After decoding, the resonators marked by "syn" are syndrome measurements to detect phase-flip errors in the qubits. An encoded qubit is teleported from KC_1 to KC_3. (b) Mapping between spin, fermions, and Majorana modes. The pairing of Majorana modes in the topologically nontrivial regime are indicated by the dotted ovals. In the topologically nontrivial phase, the MZMs are present at the ends of the chain.

$$\gamma_{n,\ell} = c_n + c_n^\dagger$$
$$\gamma_{n,r} = -ic_n + ic_n^\dagger, \tag{2}$$

where n is an integer labeling the fermions, and the ℓ, r label the two types of Majoranas, which correspond to the real and imaginary parts of the fermion operator, denoted by the left and right boxes in Fig. 1(b), respectively. Let us denote $|0_L\rangle$ a ground state of the Hamiltonian (1), taken as the state with no Majorana modes throughout the chain. The nature of the Kitaev Hamiltonian is such that applying the fermion creation operator

$$f^\dagger = \frac{1}{2}(\gamma_{1,\ell} - i\gamma_{N,r}), \tag{3}$$

consisting of two Majorana edge modes at the ends of the lattice, produces another orthogonal degenerate state.

These two states $|0_L\rangle$ and $|1_L\rangle \equiv f^\dagger|0\rangle$ are the MZM states and are used as the logical qubit states. A minimal implementation of the Kitaev chain Hamiltonian (1) consists of two fermions $N = 2$. Under the Jordan-Wigner mapping, the Hamiltonian takes a form $H = -t\sigma_1^x\sigma_2^x$ for $\Delta = t, \mu = 0$, and the two MZM states are

$$|0_L\rangle = \frac{1}{\sqrt{2}}(|++\rangle + |--\rangle)$$
$$|1_L\rangle = \frac{1}{\sqrt{2}}(|++\rangle - |--\rangle). \quad (4)$$

To encode M logical qubits, one then prepares M Kitaev chains, each with the Hamiltonian (1). Let us label the MZMs from the mth chain as

$$\gamma_\ell^{(m)} \equiv \gamma_{1,\ell}^{(m)}$$
$$\gamma_r^{(m)} \equiv \gamma_{N,r}^{(m)}, \quad (5)$$

such that we only label the leftmost and rightmost Majorana mode in the chain, which are the MZMs. An MZM, on the mth chain that is in the left- or rightmost position $\sigma \in \{\ell, r\}$, can be braided with another labeled by (m', σ'). The effect of this is to apply the unitary braid operator [53,54], defined as

$$B_{(m,\sigma)(m',\sigma')} = e^{\pi\gamma_\sigma^{(m)}\gamma_{\sigma'}^{(m')}/4} = \frac{1}{\sqrt{2}}(1 + \gamma_\sigma^{(m)}\gamma_{\sigma'}^{(m')}). \quad (6)$$

For two logical qubits, there are four MZMs, and therefore there are $\binom{4}{2} = 6$ possible braiding operations (see Fig. S4 in the Supplemental Material [55]). Because of the non-Abelian nature of MZMs, these produce gate operations on MZM states. In our circuit, we utilize the fact that braiding MZMs on the same chain produce a logical $\sqrt{Z}$ operation, and braiding adjacent MZMs on two different chains produce a logical $\sqrt{X_1X_2}$.

The standard quantum teleportation circuit consists of a sequence of Hadamard and CNOT gates [56], which are not directly available by braiding operations. To match the gates that are available with braiding operations as closely as possible, we design a modified teleportation scheme [see Fig. 2(a) and the Supplemental Material [55]]. The protocol proceeds in a similar way to the standard teleportation circuit, except that the classically transmitted quantum correction ("classical correction" for short) is done according to the modified rules shown in the classical circuit of

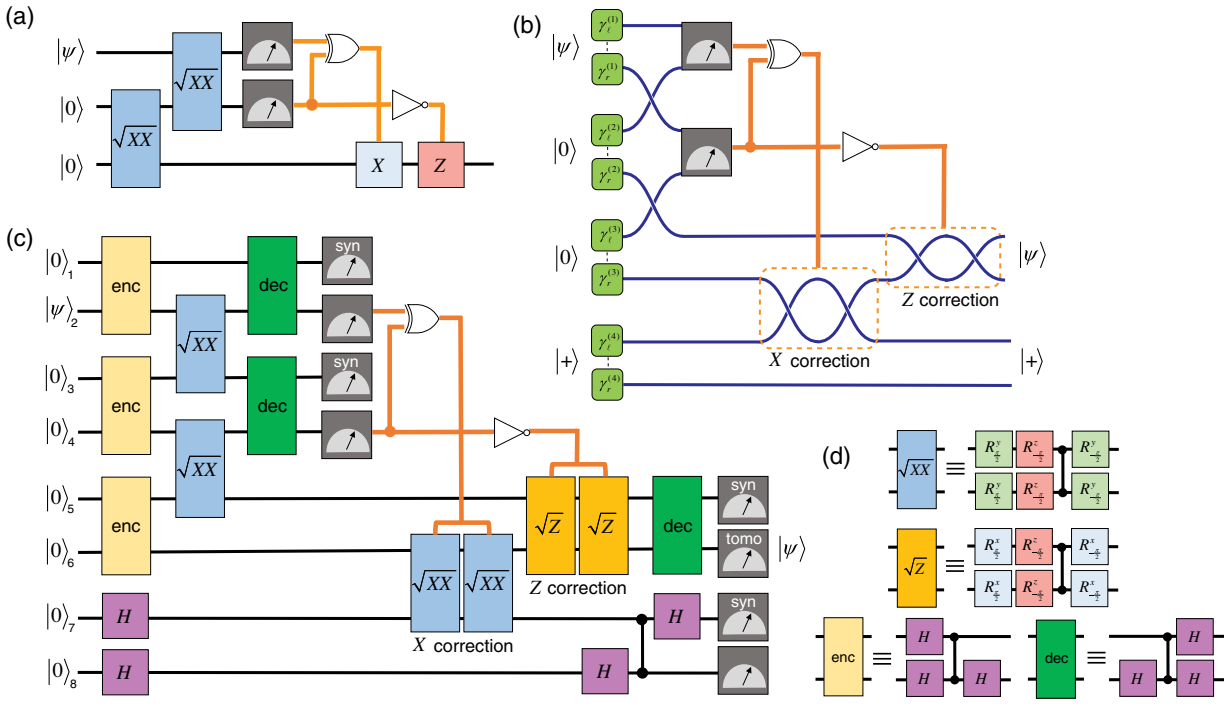

FIG. 2. Quantum circuits for simulating the teleportation of a MZM encoded qubit. (a) The modified quantum teleportation scheme. (b) The braiding sequence for MZMs that performs the quantum circuit in (a). (c) The corresponding spin-mapped qubit circuit of the MZM braiding sequence shown in (b). All measurements are performed in the $|0\rangle$, $|1\rangle$, which the exception of the measurement on qubit 6, where tomography ("tomo") is performed. The measurements marked with syn are syndrome measurements, where single-qubit phase errors are detected for a measurement outcome of $|1\rangle$. (d) The gate decompositions for the braiding, encoding, and decoding gates in (c). In all figures, $|\psi\rangle$ is the state to be teleported. Black lines connecting the quantum gates denote qubits, dark blue lines denote MZMs, and orange lines denote classical information transfer.

Fig. 2(a). Using this modified teleportation circuit, the equivalent version with MZMs can be constructed entirely using the six available braiding gates. The one gate that is not directly available as a braiding gate in the circuit of Fig. 2(a) is the X-gate for classical correction. No combination of the six braiding operations in Fig. S4 can produce a single-qubit X-gate. However, by adding an extra ancilla MZM qubit ($m = 4$) prepared in the eigenstate with $X_4 = +1$, and applying the braiding operation for the logical $\sqrt{X_3 X_4}$ twice, we can perform an X_3 gate. In this way, all gates appearing in the teleportation circuit can be performed natively using only braiding operations [Fig. 2(b)]. Using a minimal implementation of the Kitaev chain with $N = 2$ fermions, and performing a Jordan-Wigner transformation, we convert the MZM teleportation circuit [Fig. 2(b)] into the equivalent 8-qubit version as shown in Fig. 2(c).

In addition to the braiding operations, we require encoding and decoding operations to prepare the logical spin-mapped MZM qubit states of (4). The encoder takes an arbitrary qubit state and an auxiliary qubit in the state $|0\rangle$ and produces its associated logical spin-mapped MZM qubit state

$$U_{\text{enc}}|0\rangle(\alpha|0\rangle + \beta|1\rangle) = \alpha|0_L\rangle + \beta|1_L\rangle, \tag{7}$$

which can be performed using elementary gates and the definitions (4). Here α, β are arbitrary complex coefficients such that $|\alpha|^2 + |\beta|^2 = 1$. The gate decompositions for the braiding gates, encoder, and decoder $U_{\text{dec}} = U_{\text{enc}}^\dagger$ are shown in Fig. 2(d).

We choose eight adjacent qubits from a 12-qubit superconducting quantum processor [57,58] to implement the quantum circuit of Fig. 2(c). The average fidelities of single-qubit gates and the controlled-Z gate are approximately 0.9994 and 0.985, respectively. The six input states of $|0\rangle$, $|1\rangle$, $|+\rangle$, $|-\rangle$, $|+i\rangle$, $|-i\rangle$, corresponding to pairs of eigenstates of the Pauli σ^z, σ^x, σ^y operators are prepared on qubit 2 as the input state for teleportation. To perform the classical correction steps, we run four versions of the circuit with and without each of the X and Z classical correction gates. Then given a particular measurement outcome on qubits 2 and 4, the correct circuit for that outcome is selected. To perform the tomography measurement of the teleported state on qubit 6, we repeat the circuit by making measurements in the X, Y, Z basis such that the state can be tomographically reconstructed. Each of the circuit variants was run a total of 40 000 times for statistics.

Figure 3 shows the teleportation fidelities for each of the six input states. First, we average over all measurement outcomes on qubits 1,3,5,7,8, which corresponds to ignoring all error syndrome measurements and any changes in the ancilla MZM qubit. We find the average fidelity of the six states is $70.76 \pm 0.35\%$, which is above the classical limit of 2/3 [59] by 11 standard deviations. We have

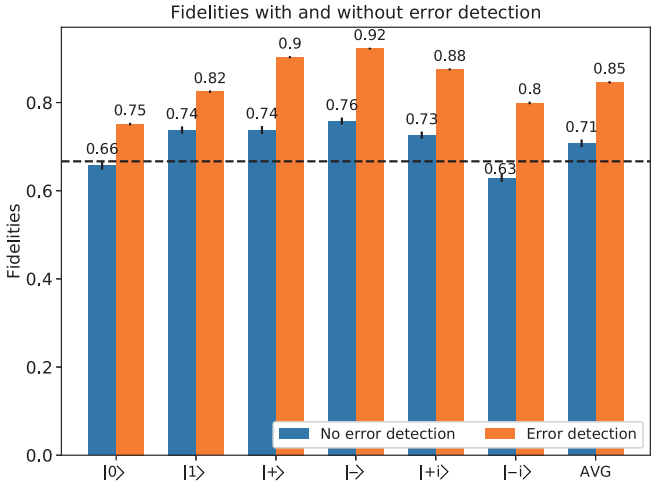

FIG. 3. Teleportation fidelities with and without error syndrome detection. The fidelity is calculated according to $F = \langle\psi|\rho|\psi\rangle$, where $|\psi\rangle = \{|0\rangle, |1\rangle, |+\rangle, |-\rangle, |+i\rangle, |-i\rangle\}$ are the ideal states to be teleported. The dashed line denotes the $F = 2/3$ threshold. The error bars denote 1 standard deviation.

performed an explicit simulation of the circuit shown in Fig. 2(c) including dephasing and gate errors and obtained good agreement between the experimentally obtained errors (see the Supplemental Material [55]). We note that the experiment further suffers from readout errors, which are expected to further degrade the theoretical fidelities. From the operations on qubit 7 and 8, it is apparent that the final state should be in the state $|00\rangle$, which is consistent with the fact that the role of these qubits is only to be in the $X = 1$ eigenstate. We experimentally obtain the probability of getting the $|00\rangle$ state is 97.98%, consistent with this expectation.

One of the benefits of encoding quantum information with MZMs is that it allows for a natural way of protecting against errors. As stated in Kiteav's original Letter [16] introducing the model (1), the MZM encoding is resilient against phase-flip errors because they correspond to nonlocal fermion interactions and bit-flip errors because they corresponds to a parity nonconserving process, which are both unlikely to occur naturally. Under the spin mapping, the protection against bit-flip errors is lost, but protection against phase-flip errors is still present (see the Supplemental Material [55]). This can be easily seen by examining the logical states after a phase flip,

$$|\tilde{0}_L\rangle = \sigma_1^z|0_L\rangle = \sigma_2^z|0_L\rangle = \frac{1}{\sqrt{2}}(|-+\rangle + |+-\rangle)$$
$$|\tilde{1}_L\rangle = \sigma_1^z|1_L\rangle = -\sigma_2^z|1_L\rangle = \frac{1}{\sqrt{2}}(|-+\rangle - |+-\rangle). \tag{8}$$

The states $|\tilde{0}_L\rangle$, $|\tilde{1}_L\rangle$ span an orthogonal subspace to that spanned by the logical states and are produced when any single-qubit phase error occurs. Using the relation

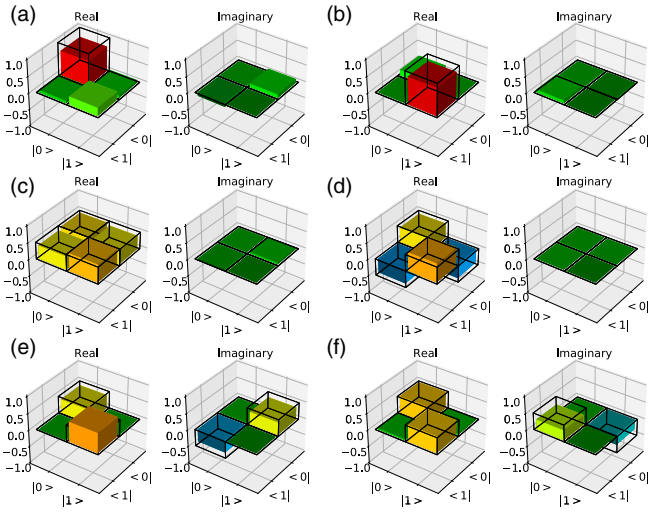

FIG. 4. Tomography of the final teleported state after using the error syndrome measurements. The initial state prepared on qubit 2 is (a) $|0\rangle$, (b) $|1\rangle$, (c) $|+\rangle$, (d) $|-\rangle$, (e) $|+i\rangle$, (f) $|-i\rangle$. Frames show ideal teleportation states; colored bars show the experimentally determined state.

$$U_{\mathrm{dec}}(\alpha|\tilde{0}_L\rangle + \beta|\tilde{1}_L\rangle) = |1\rangle(\alpha|0\rangle + \beta|1\rangle), \tag{9}$$

we can see that the measurement outcomes of $|1\rangle$ on the auxiliary qubits allow one to deduce that a phase-flip error has occurred on any of the qubits. This constitutes an error detecting code [5,60–62], which can be used to passively improve the fidelity of the circuit by discarding any results where errors have occurred [45,46,48–51].

Figure 3 shows the teleportation fidelities using the error syndrome measurements on qubits 1,3,5,7. A measurement of the state $|1\rangle$ on any of these qubits signals that at least one phase-flip error has occurred, such that it is removed from the data set. All results on the ancilla qubit 8 are included. We observe that the fidelities of the telportation improve significantly for all states, with an average of $84.60 \pm 0.11\%$ for the six states. This further increases the average fidelity beyond the classical bound by over 163 standard deviations. The final teleported state for the error syndrome improved state is tomographically reconstructed using a maximum likelihood estimator of the density matrix and shown in Fig. 4. We see that the states of the six input states are very well reproduced, demonstrating that the teleportation is being performed correctly over the six mutually unbiased basis states.

In summary, we have performed a quantum simulation of the teleportation of a qubit encoded as the MZM states of the Kitaev chain. The teleportation circuit is performed entirely using braiding operations of the MZMs, including the quantum gates for classical correction. In our teleportation circuit, we were careful to be faithful to the braiding process of the MZMs in the sense that no gate simplifications were performed in the circuit Fig. 2(c). This demonstrates via an equivalent spin encoding that a nontrivial quantum circuit can be performed using a topological quantum computing sequence using braids. In addition, numerous demonstrations of teleportation have been performed to date in qubit [63–70] and higher dimensional systems [71–75], but never in combination with quantum error correction. Purely from the perspective of the spin formulation, our work can also be viewed as a demonstration of an encoded qubit teleportation.

The benefit of the MZM encoding in the original fermion model is protection against both bit- and phase-flip errors [16]. By performing the spin mapping, the protection against bit-flip errors is lost, as evident by examining the states (4). However, the protection against phase-flip errors is still present, and we explicitly demonstrated the enhancement in fidelity of the teleportation by postselecting states without detected errors. Thus, our results also indicate the feasibility of phase error protection in MZM-based topological quantum computing. Longer chains are expected to enhance the phase error protection, but will make the states more susceptible to bit-flip errors due to a higher probability of an error occurring somewhere on the chain. Thus, while we do not expect that the spin encoding benefits from larger N, in the original fermion model we expect that the logical states should have an enhanced protection. In addition to the error detection performed here, with the addition of a topological gap to energetically separate the logical space from the error space, errors could be actively suppressed, further improving the error protection.

The authors thank the Laboratory of Microfabrication, University of Science and Technology of China, Institute of Physics CAS, and National Center for Nanoscience and Technology for supporting the sample fabrication. The authors also thank QuantumCTek Co. Ltd. for supporting the fabrication and the maintenance of room-temperature electronics. This research was supported by the National Key Research and Development Program of China (Grants No. 2017YFA0304300), NSFC (Grants No. 11574380, No. 11905217), the Chinese Academy of Science and its Strategic Priority Research Program (Grant No. XDB28000000), the Science and Technology Committee of Shanghai Municipality, Shanghai Municipal Science and Technology Major Project (Grant No. 2019SHZDZX01), and Anhui Initiative in Quantum Information Technologies. The work of T. B. is supported by the National Natural Science Foundation of China (62071301); State Council of the People's Republic of China (D1210036A); NSFC Research Fund for International Young Scientists (11850410426); NYU-ECNU Institute of Physics at NYU Shanghai; the Science and Technology Commission of Shanghai Municipality (19XD1423000); the China Science and Technology Exchange Center (NGA-16-001). The work of H.-L. H. was supported by the Open Research Fund from

State Key Laboratory of High Performance Computing of China (Grant No. 201901-01), NSFC (Grant No. 11905294), and China Postdoctoral Science Foundation.

H.-Liang Huang, M. Narożniak, and F. Liang contributed equally to this work.

*These authors contributed equally to this work.
†xbzhu16@ustc.edu.cn

[1] P. W. Shor, in *Proceedings of 37th Conference on Foundations of Computer Science* (IEEE, New York, 1996), pp. 56–65.
[2] D. Gottesman, Phys. Rev. A **57**, 127 (1998).
[3] A. M. Steane, Nature (London) **399**, 124 (1999).
[4] D. Aharonov and M. Ben-Or, arXiv:quant-ph/9906129.
[5] J. Preskill, in *Introduction to Quantum Computation and Information* (World Scientific, Singapore, 1998), pp. 213–269.
[6] D. Gottesman, arXiv:0904.2557.
[7] S. J. Devitt, W. J. Munro, and K. Nemoto, Rep. Prog. Phys. **76**, 076001 (2013).
[8] E. T. Campbell, B. M. Terhal, and C. Vuillot, Nature (London) **549**, 172 (2017).
[9] A. Y. Kitaev, Ann. Phys. (Amsterdam) **303**, 2 (2003).
[10] M. Freedman, A. Kitaev, M. Larsen, and Z. Wang, Bull. Am. Math. Soc. **40**, 31 (2003).
[11] J. Preskill, *Lecture Notes on Quantum Computation* (1998), Chap. 5, http://www.theory.caltech.edu/~preskill/ph229/#lecture.
[12] C. Nayak, S. H. Simon, A. Stern, M. Freedman, and S. D. Sarma, Rev. Mod. Phys. **80**, 1083 (2008).
[13] J. K. Pachos, *Introduction to Topological Quantum Computation* (Cambridge University Press, Cambridge, 2012).
[14] S. D. Sarma, M. Freedman, and C. Nayak, npj Quantum Inf. **1**, 15001 (2015).
[15] V. Lahtinen and J. K. Pachos, SciPost Phys. **3**, 021 (2017).
[16] A. Y. Kitaev, Phys. Usp. **44**, 131 (2001).
[17] J. Alicea, Rep. Prog. Phys. **75**, 076501 (2012).
[18] M. Leijnse and K. Flensberg, Semicond. Sci. Technol. **27**, 124003 (2012).
[19] C. Beenakker, Annu. Rev. Condens. Matter Phys. **4**, 113 (2013).
[20] R. t. Lutchyn, E. Bakkers, L. P. Kouwenhoven, P. Krogstrup, C. Marcus, and Y. Oreg, Nat. Rev. Mater. **3**, 52 (2018).
[21] R. Willett, J. P. Eisenstein, H. L. Störmer, D. C. Tsui, A. C. Gossard, and J. H. English, Phys. Rev. Lett. **59**, 1776 (1987).
[22] S. D. Sarma, M. Freedman, and C. Nayak, Phys. Rev. Lett. **94**, 166802 (2005).
[23] R. L. Willett, L. N. Pfeiffer, and K. West, Proc. Natl. Acad. Sci. U.S.A. **106**, 8853 (2009).
[24] R. L. Willett, C. Nayak, K. Shtengel, L. N. Pfeiffer, and K. W. West, Phys. Rev. Lett. **111**, 186401 (2013).
[25] V. Mourik, K. Zuo, S. M. Frolov, S. Plissard, E. P. Bakkers, and L. P. Kouwenhoven, Science **336**, 1003 (2012).
[26] R. M. Lutchyn, J. D. Sau, and S. Das Sarma, Phys. Rev. Lett. **105**, 077001 (2010).
[27] Y. Oreg, G. Refael, and F. von Oppen, Phys. Rev. Lett. **105**, 177002 (2010).
[28] R. A. Sola and L. Kouwenhoven, Phys. Today **73**, No. 6, 44 (2020).
[29] H.-L. Huang, D. Wu, D. Fan, and X. Zhu, Sci. Chin. Inf. Sci. **63**, 180501 (2020).
[30] J.-S. Xu, K. Sun, Y.-J. Han, C.-F. Li, J. K. Pachos, and G.-C. Guo, Nat. Commun. **7**, 13194 (2016).
[31] J.-S. Xu, K. Sun, J. K. Pachos, Y.-J. Han, C.-F. Li, and G.-C. Guo, Sci. Adv. **4**, eaat6533 (2018).
[32] C.-Y. Lu, W.-B. Gao, O. Gühne, X.-Q. Zhou, Z.-B. Chen, and J.-W. Pan, Phys. Rev. Lett. **102**, 030502 (2009).
[33] J. Pachos, W. Wieczorek, C. Schmid, N. Kiesel, R. Pohlner, and H. Weinfurter, New J. Phys. **11**, 083010 (2009).
[34] Y.-P. Zhong, D. Xu, P. Wang, C. Song, Q. J. Guo, W. X. Liu, K. Xu, B. X. Xia, C.-Y. Lu, S. Han, J.-W. Pan, and H. wang, Phys. Rev. Lett. **117**, 110501 (2016).
[35] H.-N. Dai, B. Yang, A. Reingruber, H. Sun, X.-F. Xu, Y.-A. Chen, Z.-S. Yuan, and J.-W. Pan, Nat. Phys. **13**, 1195 (2017).
[36] C. Song, D. Xu, P. Zhang, J. Wang, Q. Guo, W. Liu, K. Xu, H. Deng, K. Huang, D. Zheng *et al.*, Phys. Rev. Lett. **121**, 030502 (2018).
[37] C. Liu, H.-L. Huang, C. Chen, B.-Y. Wang, X.-L. Wang, T. Yang, L. Li, N.-L. Liu, J. P. Dowling, T. Byrnes *et al.*, Optica **6**, 264 (2019).
[38] Y. Tserkovnyak and D. Loss, Phys. Rev. A **84**, 032333 (2011).
[39] A. Mezzacapo, J. Casanova, L. Lamata, and E. Solano, New J. Phys. **15**, 033005 (2013).
[40] C. H. Bennett, G. Brassard, C. Crépeau, R. Jozsa, A. Peres, and W. K. Wootters, Phys. Rev. Lett. **70**, 1895 (1993).
[41] M. H. Freedman, M. Larsen, and Z. Wang, Commun. Math. Phys. **227**, 605 (2002).
[42] A. Stern and N. H. Lindner, Science **339**, 1179 (2013).
[43] X.-C. Yao, T.-X. Wang, H.-Z. Chen, W.-B. Gao, A. G. Fowler, R. Raussendorf, Z.-B. Chen, N.-L. Liu, C.-Y. Lu, Y.-J. Deng *et al.*, Nature (London) **482**, 489 (2012).
[44] D. Nigg, M. Mueller, E. A. Martinez, P. Schindler, M. Hennrich, T. Monz, M. A. Martin-Delgado, and R. Blatt, Science **345**, 302 (2014).
[45] J. Kelly, R. Barends, A. G. Fowler, A. Megrant, E. Jeffrey, T. C. White, D. Sank, J. Y. Mutus, B. Campbell, Y. Chen *et al.*, Nature (London) **519**, 66 (2015).
[46] A. D. Córcoles, E. Magesan, S. J. Srinivasan, A. W. Cross, M. Steffen, J. M. Gambetta, and J. M. Chow, Nat. Commun. **6**, 6979 (2015).
[47] N. Ofek, A. Petrenko, R. Heeres, P. Reinhold, Z. Leghtas, B. Vlastakis, Y. Liu, L. Frunzio, S. Girvin, L. Jiang *et al.*, Nature (London) **536**, 441 (2016).
[48] N. M. Linke, M. Gutierrez, K. A. Landsman, C. Figgatt, S. Debnath, K. R. Brown, and C. Monroe, Sci. Adv. **3**, e1701074 (2017).
[49] M. Takita, A. W. Cross, A. D. Córcoles, J. M. Chow, and J. M. Gambetta, Phys. Rev. Lett. **119**, 180501 (2017).
[50] S. Rosenblum, P. Reinhold, M. Mirrahimi, L. Jiang, L. Frunzio, and R. Schoelkopf, Science **361**, 266 (2018).
[51] R. Harper and S. T. Flammia, Phys. Rev. Lett. **122**, 080504 (2019).
[52] C. K. Andersen, A. Remm, S. Lazar, S. Krinner, N. Lacroix, G. J. Norris, M. Gabureac, C. Eichler, and A. Wallraff, Nat. Phys. **16**, 875 (2020).

[53] C. Nayak and F. Wilczek, Nucl. Phys. **B479**, 529 (1996).
[54] D. A. Ivanov, Phys. Rev. Lett. **86**, 268 (2001).
[55] See Supplemental Material at http://link.aps.org/supplemental/10.1103/PhysRevLett.126.090502 for braiding operations, modified teleportation scheme, and experimental details.
[56] M. A. Nielsen and I. Chuang, *Quantum Computation and Quantum Information*, 10th Anniversary ed. (Cambridge University Press, Cambridge, England, 2011), https://doi.org/10.1017/CBO9780511976667.
[57] M. Gong, M.-C. Chen, Y. Zheng, S. Wang, C. Zha, H. Deng, Z. Yan, H. Rong, Y. Wu, S. Li *et al.*, Phys. Rev. Lett. **122**, 110501 (2019).
[58] H.-L. Huang, Y. Du, M. Gong, Y. Zhao, Y. Wu, C. Wang, S. Li, F. Liang, J. Lin, Y. Xu *et al.*, arXiv:2010.06201.
[59] S. Massar and S. Popescu, Phys. Rev. Lett. **74**, 1259 (1995).
[60] L. Vaidman, L. Goldenberg, and S. Wiesner, Phys. Rev. A **54**, R1745 (1996).
[61] M. Grassl, T. Beth, and T. Pellizzari, Phys. Rev. A **56**, 33 (1997).
[62] S. P. Jordan, E. Farhi, and P. W. Shor, Phys. Rev. A **74**, 052322 (2006).
[63] D. Bouwmeester, J.-W. Pan, K. Mattle, M. Eibl, H. Weinfurter, and A. Zeilinger, Nature (London) **390**, 575 (1997).
[64] D. Boschi, S. Branca, F. De Martini, L. Hardy, and S. Popescu, Phys. Rev. Lett. **80**, 1121 (1998).
[65] M. Riebe, H. Häffner, C. Roos, W. Hänsel, J. Benhelm, G. Lancaster, T. Körber, C. Becher, F. Schmidt-Kaler, D. James *et al.*, Nature (London) **429**, 734 (2004).
[66] M. Barrett, J. Chiaverini, T. Schaetz, J. Britton, W. Itano, J. Jost, E. Knill, C. Langer, D. Leibfried, R. Ozeri *et al.*, Nature (London) **429**, 737 (2004).
[67] X.-S. Ma, T. Herbst, T. Scheidl, D. Wang, S. Kropatschek, W. Naylor, B. Wittmann, A. Mech, J. Kofler, E. Anisimova *et al.*, Nature (London) **489**, 269 (2012).
[68] M. Baur, A. Fedorov, L. Steffen, S. Filipp, M. P. Da Silva, and A. Wallraff, Phys. Rev. Lett. **108**, 040502 (2012).
[69] W. Pfaff, B. J. Hensen, H. Bernien, S. B. van Dam, M. S. Blok, T. H. Taminiau, M. J. Tiggelman, R. N. Schouten, M. Markham, D. J. Twitchen *et al.*, Science **345**, 532 (2014).
[70] J.-G. Ren, P. Xu, H.-L. Yong, L. Zhang, S.-K. Liao, J. Yin, W.-Y. Liu, W.-Q. Cai, M. Yang, L. Li *et al.*, Nature (London) **549**, 70 (2017).
[71] A. Furusawa, J. L. Sørensen, S. L. Braunstein, C. A. Fuchs, H. J. Kimble, and E. S. Polzik, Science **282**, 706 (1998).
[72] Q. Zhang, A. Goebel, C. Wagenknecht, Y.-A. Chen, B. Zhao, T. Yang, A. Mair, J. Schmiedmayer, and J.-W. Pan, Nat. Phys. **2**, 678 (2006).
[73] H. Krauter, D. Salart, C. Muschik, J. M. Petersen, H. Shen, T. Fernholz, and E. S. Polzik, Nat. Phys. **9**, 400 (2013).
[74] X.-L. Wang, X.-D. Cai, Z.-E. Su, M.-C. Chen, D. Wu, L. Li, N.-L. Liu, C.-Y. Lu, and J.-W. Pan, Nature (London) **518**, 516 (2015).
[75] Y.-H. Luo, H.-S. Zhong, M. Erhard, X.-L. Wang, L.-C. Peng, M. Krenn, X. Jiang, L. Li, N.-L. Liu, C.-Y. Lu, A. Zeilinger, and J.-W. Pan, Phys. Rev. Lett. **123**, 070505 (2019).